THE EMBEDDED POLYMERIC OPTICAL FIBER (POF) IN 3D COMPOSITE FOR HEALTH MONITORING

Tamer Hamouda[12], **Abdel-Fattah M. Seyam**[1], **Kara Peters**[2]
[1] *Textile Research Division, National Research Centre, Dokki, Cairo 12622, Egypt*
[2] *North Carolina State University, Raleigh, NC 27695, USA*
tehamoud@ncsu.edu

ABSTRACT
Since most of structure deals directly with people, there is a strong need for a reliable structural health monitoring system (SHM) that can detect and locate the internal and unseen damages. In this research, 3D composite samples with embedded POFs with different parameters were fabricated. OTDR was connected to the embedded POF to measure the signal attenuation. POF Signal were collected during the preform manufacturing process, VARTM process, after curing and under different bending loads and repeated impact tests. Results showed good response of embedded POF sensor under different loading loads and under repeated impacts.

Key Words: 3D WOVEN FABRIC, POLYMER OPTICAL FIBER, OTDR, SHMS

1. INTRODUCTION
Engineered infrastructure such as dams, bridges, and skyscrapers are heavy, expensive and need to be maintained from time to time. Nevertheless, any construction has a lifetime which mainly depends it is location and the surrounding atmospheres such as earthquakes, tornadoes. [1]. Thus, structural health monitoring systems (SHM) are must in order to detect any changes that may occurred to the structure, which present an indication to the damage and/or structural failure [2-3]. SHMs include sensing object whether electrical or optical sensors, data collecting unit, and data analysis systems [4]. Sudden structure failure may happen due to the growth of undetected hidden and unnoticeable damage. Thus, reliable SHM system that able to detect the internal failure and locate the failure location is desired [5].

Advantages of textile composites such as light weigh, high strength to weigh ration have led to the utilization of composite in many applications such as aircrafts, automobile, military, wind turbine blade [6]. In addition, three dimensional woven preforms used in composite materials permit optical fiber sensors to be integrated into 3D woven preform during the weaving manufacturing process [7]. Nonwoven preform, stack of 2D woven, and 3D woven preform are different technologies that is used to create 3D textile structures. 3D orthogonal woven preforms are known for their higher resistance to crack propagation, eliminate delamination, faster in resin transfer, and higher fiber volume fraction [8-10] Composites' manufacturing parameters, internal strain, Impact damage and bending during the composite manufacturing process can be monitored using embedded optics sensors into textile structures [11-13]. Polymeric optical fiber (POF) sensors carry many advantageous such as high numerical aperture, flexibility and easy to handle, inexpensive, easy to splice and cleave, do not require protective layer, and can handle high tensile strain and high fracture toughness [14]. Optical Time Domain Reflectometer (OTDR) is used to measure optical fiber transmission signal losses, determine the defects' location, and also measure optical fiber length [15]. In this research OTDR is also used to monitor optical fibers signals during the woven preform fabrication, composite fabrication, under mechanical tests [16]. POF sensors were embedded into 3D orthogonal preform during the preform fabrication.

2. EXPERIMENTATION

2.1 Materials and Methd

The used POF specifications are; core diameter of 62.5 µm, and cladding diameter of 750 µm. POF core and cladding are made of perfluorinated polymer (PF) (Polyperfluoro-butenyvinyleether). 3D orthogonal woven preform were made of E-glass fiber, supplied by PPG Industries. The linear densities of the used E-glass fibers are 735 (g/km or tex) for the x-yarn, 2275 (g/km or tex) for the y-yarn, and 276 (g/km or tex) for the z- yarn, respectively. Figure 1 shows 3D orthogonal woven preform with x-, y-, and z-yarns identification.

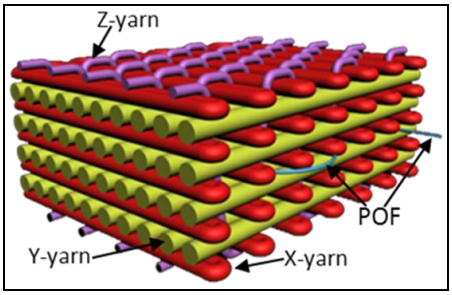

Figure 1. 3D orthogonal woven preform (Y-yarn (yellow), x-yarn (red), z-yarn (purple), and POF (blue)) [17]

2.2. Experimental Design

Table 1 depicts experimental design of prepared 3D orthogonal woven composite for bending and impact tests. Three variables namely number of y-yarn layers (2, 3, and 4 layers), Two x-yarn density/layer were used (1.57, 4.72 Wefts/cm/layer), and increment bending load of 5 levels that differ in value depending on sample thickness or number of layers.

Table 1 Sample Specifications

Sample ID	Weft Density (Wefts/cm/layer)	Warp Layers (Weft Layers)
A	1.57	2 (3)
B	4.72	2 (3)
C	1.57	3 (4)
D	4.72	3 (4)
E	1.57	4 (5)
F	4.72	4 (5)

2.3. Bending testing and evaluation

Three-point bending test was conducted using TESTRESOUCES (130Q1000 load frame). The bending test machine is a customized machine with dual column load frame with 500 mm clearance between the two columns to wide specimen. The span length ranges between 30 and 470 mm. The bending test conducted at speed of 4 mm/min and span length of 65 mm. The specimen length was 45 cm in the x-direction, which is the direction of the POF, and 15 cm width (figure 6). One protruded end of the POF was connected to the OTDR to measure the backscattering level and induced signal attenuation under applied load and after releasing the load.

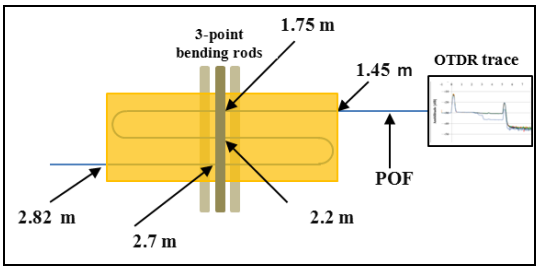

Figure 6. schematic diagram of impact test [19]

2.4. Impact Testing and Evaluation

Instron impact tester model CEAST 9310, which is low energy impact tester, was used to impact each sample repeatedly for up to 30 impacts or until the POF lost its entire dynamic range whichever reaches first. Each sample was impacted with energy of 9 Joules using 1 Kg mass and 3.71 m/s velocity. One protruded end of POF was connected to the OTDR to assess the signal loss before the impact and after each impact. Figure 3 shows schematic of a sample prepared for the test and the impact location, which is approximately in the middle of the POF length (about 2.5 meters from the OTDR front panel connector).

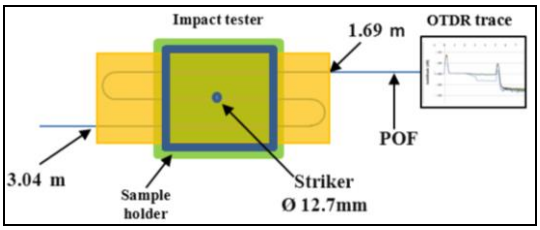

Figure 7. schematic diagram of impact test [19]

3. RESULTS AND DISCUSSION

3.1 Attenuation measurement during fabrication

Backscattering level (using OTDR) was measured for as supplied POF (control). The backscattering level was recorded after weaving POF into 3D preform, after applying vacuum for, and after resin infusion. This technique will allow for the identification of the cause of signal loss if any. Figure 8 depict the typical OTDR trace of sample E which consists of 4 x-yarn layers with x-yarn density of 1.57 x-yarns/cm/layer). The embedded length of POF sensor was 1.369 m, whereas POF entered the 3D preform at length of 1.452 m and exited the preform at length of 2.821 m. Noticeable drop on the backscattering level at distance of 2.13 m occurred after applying 100 Kpa vacuum pressure. This drop indicates significant effect of the vacuum pressure on POF resulting from fiber distortion due to micro bending effect, which was not recovered after resin curing. Results also indicates that weaving process didn't cause any damage to the POF sensor.

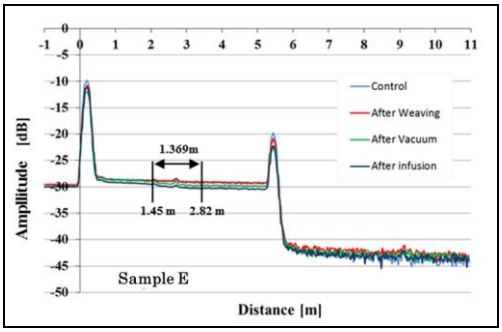

Figure 8. Backscattering of embedded POF into composite sample for different fabrication processes.

Compiled signal attenuation data after each process of composite fabrication process is shown in figure 9 shows. Results showed that all embedded POF into samples made of 2 y-yarn layers showed attenuation after weaving process (0.14 dB-0.22 dB) while POF in samples of 3 and 4 y-yarn layers did not exhibit significant signal attenuation. This result may have attributed to that samples made of 2 y-yarn layers exhibit open and flexible structure that may cause the POF to be easily distorted at the contact points with preform yarns and during sample handling. Waviness of POF in such structure was noticed. The results of signal attenuation after vacuum application indicate that open structure samples with low number of y-yarn layers and x-yarn densities did not provide support for the POF a matter that caused more signal loss. However, after 24 hours from resin infusion the signal attenuation of all samples is about the same, which is evidence of distortion recovery of the POF.

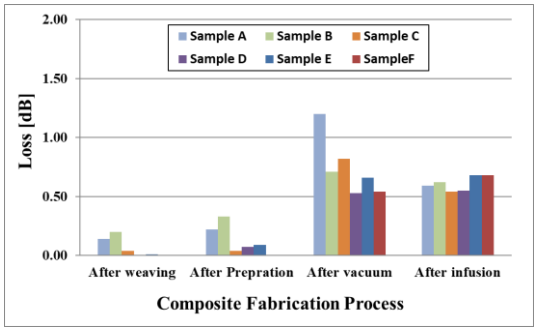

Figure 9. Signal attenuation of embedded POF during the fabricating process

3.2. Attenuation of POF Signal due to Bending

One protruded end of the embedded POF was connected to OTDR and backscattering and signal attenuation was collected while 3D composite samples experienced different bending loads. Bending load was applied to the required level, then the test was paused and backscattering signal was collected. The load was released and signal was measured. Signal was also measured for all samples at failure load and after releasing the load.

OTDR signal traces of embedded POF in composite of 4 y-yarn layers with x-yarn density 1.57 (sample E) under different bending loads are shown in figure 10. Results revealed that under bending load of 605 N, no signal loss was recorded. Loads/strain 1,210 N/1.6%, 1,815 N/2.3%, 2,303 N/2.9%, and 2,460 N/3.0% caused drops in POF backscattering at three different locations (1.75 m, 2.24 m, and 2.70 m), which present the three contact points between composite sample and the upper rod of bending fixture. Signal attenuation is caused by bending and flattening of the POF at these three points. Results indicate that the change in cross-section shape of the POF leads to change in the refractive index of POF, which leads to that drop in the backscattering level at these three locations. when 2,460 N load is applied on the composite sample (breaking load) it was noticed that signal attenuation of POF sensor is very high. The recorded OTDR's signal indicate loss and reflection, which is a clear indication of structure damages. This may occur due to necking in POF sensor under very high bending moment. Backscattering data and signal loss were also collected after releasing each load. Figure 11 shows the backscattering level after removing the loads. OTDR trace results showed a significant recovery of POF after removing the bending load up to 2,303 N. Results also showed that backscattering level returned to its original levels after removing the loads. After releasing the breaking load of 2,460 N, Backscattering trace showed that the reflection part of the signal has been removed and the signal loss of POF decreased from 10.43 dB to 2.9 dB from 10.4 dB.

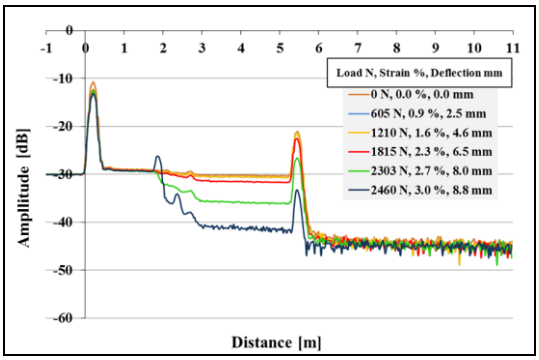

Figure 10. Backscattering of sample E made of 4 y-yarn layers and density of 1.57 x-yarn/cm/layer under different bending loads.

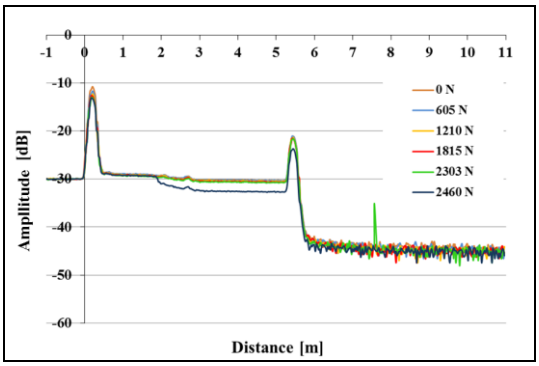

Figure 11. Backscattering of sample E made of 4 y-yarn layers and density of 1.57 x-yarn/cm/layer after removing different bending loads

3.3. Attenuation of POF Signal due to Impact

The POFs embedded in samples D and F maintained dynamic range of 9 dB and 11 dB, respectively, after 30 impacts. The POFs in samples A, B, C, and E lost their dynamic range (not capable of sensing any more due to damage) after 3, 9, 3, and 14 impacts, respectively. OTDR traces of the POF embedded in sample A is shown in figure 12. Figure indicates that the whole dynamic range was lost after the third repeated impact. Even though the signal loss was significant after the first impact. This can be attributed to the structure of the sample, whereas this sample exhibit the least fiber volume fraction, lowest number of warp/weft layers, and lowest weft density which makes it vulnerable to impact. The impact damage was transferred to the POF, which means that the signal loss of the POF is proportional to the occurred damage. Figure 13 shows the corresponding images of the sample after each impact and it can be noticed that the damaged area is increasing with the number of repeated impacts.

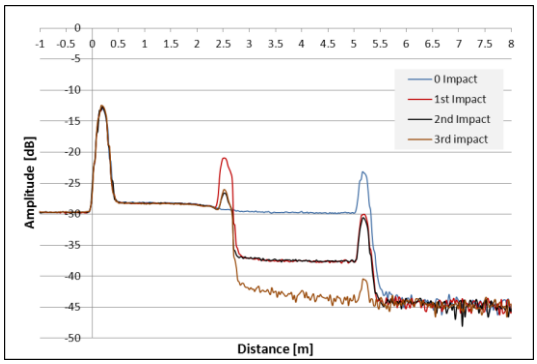

Figure 12. Signal traces of POF embedded in sample A before and after impact

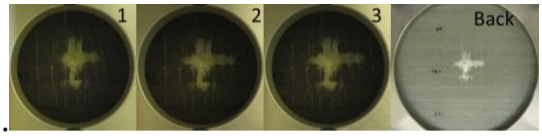

Figure 13. Images of sample A after impact 1, 2, and 3 and the back of the sample after impact.

OTDR traces of the POF embedded in samples D and F are shown in Figure 14 and 15. It can be seen from the figure that the POF maintained 11 dB from its dynamic range after 30 impacts. The signal loss value was gradually increasing with the number of impacts. Unlike sample A, samples D and F possesses the highest fiber volume fraction, highest number of warp/weft layers, and highest weft density. Such structure provided high resistance to the impact energy. The damage of the sample after each impact was gradually transferred to the POF. Again, this is a good indication that the POF sensing is proportional to the sample damage. Figure 8 shows the corresponding images of the sample after each impact and it can be seen that the damaged area is increasing with the number of impacts.
Similar results were noticed for samples B, C, D, and E. Generally, the signal loss in these samples was also proportional to the degree of damage assessed visually and the damage level is a function of the structure parameters.

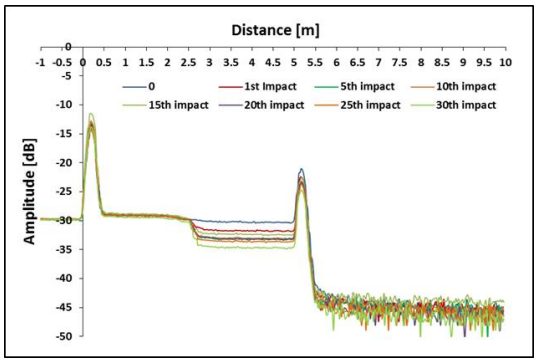

Figure 14. Signal traces of POF embedded in sample D before and after 30 impacts

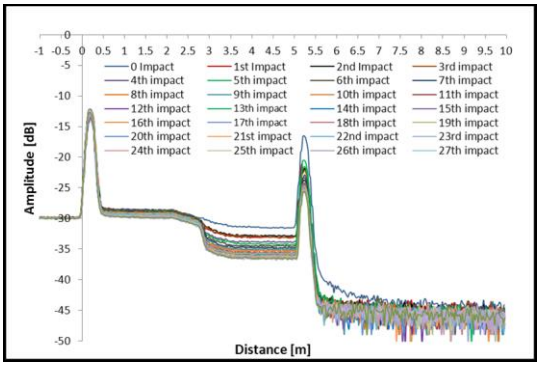

Figure 15. Signal traces of POF embedded in sample F before and after 30 impacts (traces of impacts 28, 29, and 30 are very close to trace of impact 27)

Figure 16. Images of sample F after each of 30 impacts and the sample image of the back after impact 30.

All acquired results from OTDR prove that the signal loss is related to the damage of the composite samples; as the damaged area is increased and reach the other side of the sample (back), the signal attenuation increases. However, this assessment is subjective and the mechanical performance cannot be quantified.

4. CONCLUSİON

3D weaving machine and VARTM technique were used to manufacture the composite samples. OTDR was connected to the embedded POF to measure the signal attenuation. POF Signal were collected during the preform manufacturing process, VARTM process, after curing and under different bending loads and repeated impact tests. It was found that the weaving process has no significant effect of POF signal. Very small attenuation in POF signal was recorded during the VARTM process. Very good respond of the POF were recorded under different bending loads and after releasing the loads. Also, damage due to repeated impact was indicated by signal attenuation for the low weft densities' samples.

5. REFERENCES

1. Chang P., Flata A., Liu S.C., Review Paper: Health Monitoring of Civil Infrastructure". *Structural Health Monitoring*, 2003, Vol.2, No.3, 0257–267.
2. Housner G. W., Bergman L. A., Caughey T.K., Chassiakos A.G., Claus R.O., Masri S.f., Skelton, R. E., Soon, T. T., Spencer, B. F., Yao J.T.P., Structural Control: Past, Present, And Future, *Journal Of Engineering Mechanics,* Vol.123, No.9, 897-971.
3. Zhan-feng G., Yan-liang D., Bao-Chen S., Xiu-mei J., Strain monitoring of railway bridges using optic fiber sensors, *Journal of quality in Maintenance Engineering,* 2007, Vol.13, No.2, 186-197.
4. Li H., Li D., Song G., Recent applications offiber optic sensors to health monitoring in civil engineering, *Engineering Structures*, 2004, Vol.26, No.11, 1647–1657.
5. Mal A., Ricci F., Banerjee S., Shih F. A., Conceptual Structural Health Monitoring system based on Vibration and wave Propagation, *Structural Health Monitoring* 2005, Vol.4, No.3, 283-293.
6. Tao X. M, Integration of Fiber-optic Sensors in Smart Textile Composites: Design and Fabrication, *Journal of Textile Institute,* 2000, Vol.91, No.3, 448-459.
7. Bogdanovich, A., E., Wigent III, D., E., Whitney, T., J., Fabrication of 3-D Woven Preforms and Composites with Integrated Fiber Optic Sensors, *SAMPE Journal* 2003, Vol.39, No.4, 6-15.
8. Mohamed, T. S., Johnson, C. Rizkalla, S., Behavior of Three-Dimensionally Woven

Glass Fiber Reinforced Polymeric Bridge Deck, *Composites Research Journal*, 2007, Vol.1, No.2, 27-42.
9. Mohamed M., Dickinson L., Singletary J., Lienhart B., A new generation of 3D woven fabric preforms and composites, *SAMPE Journal*, 2001, Vol.37, No.3, 8-17.
10. Bogdanovich A., Advancements In Manufacturing And Applications Of 3-D Woven Preforms And Composites, *16th International conference on composite materials*, Kyoto, Japan, 2007.
11. Kang H., Kang D., Hong C., Kim C., Monitoring of Fabrication strain and temperature During Composite cure Using Fiber Optic Sensors, *Nondestructive Evaluation of Materials and Composites*, Vol.4336, 211-218.
12. 12. Kosaka T., Osaka K., Nakakita S. Fukuda T., Fiber optic strain monitoring of textile GFRP during RTM molding and fatigue tests by using embedded FBG sensors, *Smart Structures and Materials*, 2003, Vol.5056, 73-80.
13. Rogers, C. A., Intelligent Material Systems and Structures, *US/Japan Working on Smart/Intelligent Materials and Systems*, 1990, 11–18.
14. Peters, K., Polymer optical fiber sensors-a review, *Smart Materials And Structures*, 2010, Vol.20, No.1, 13002-17
15. Liehr, S., Nother,N., Krebber, K., Incoherent optical frequency domain reflectometry and distributed strain detection in polymer optical fibers, *Meas. Sci. Technol*, 2010, Vol.21, No.1, 1-4.
16. Anderson, D., Johnson, L., Bell, F., Troubleshooting Optical-Fiber Networks. Understanding and Using your Optical Time-Domain Reflectometer, *San Diego, California : Elsevier Academic Press*, 2004.
17. Hamouda, T., Peters, K., Seyam, A. M., Effect of Resin Type on Signal Integrity of an Embedded Perfluorinated Polymer Optical Fiber, *Journal of Smart Materials and Structures*, 2012, Vol.21, No.5, 1-8.
18. Seyam, A.M. Hamouda, T., Smart Textiles: Evaluation of Optic Fibers as Embedded Sensors for Structure Health Monitoring of Fiber Reinforced Composites, *Journal of the Textile Institute*, 2013, Vol.104, No.8, 892-899.
19. Hamouda, T.M., Smart Textiles: Evaluation of Fiber Optic Sensors Embedded in 3D Orthogonal Woven Composites and their Impact on the Host Structure Integrity, Ph.D. Thesis, NC State University, Raleigh, NC, 2002 (under direction of Seyam & Peters).
20. Hamouda T., Seyam, M. A., Peters K., Evaluation of the integrity of 3D orthogonal woven composites with embedded polymer optical fibers, *Composites Part B*, 2015, Vol.78, 79-85.